Available online at www.sciencedirect.com
SCIENCE DIRECT®
Journal of Catalysis 236 (2005) 122–128
JOURNAL OF CATALYSIS
www.elsevier.com/locate/jcat

Liquid-phase isophorone oxide rearrangement over mesoporous Al-MCM-41 materials

Rafael van Grieken, David P. Serrano, Juan Antonio Melero [*], Alicia García

Chemical and Environmental Engineering Group, ESCET, Rey Juan Carlos University, C/Tulipán s/n, 28933 Móstoles, Spain

Received 22 July 2005; revised 21 September 2005; accepted 26 September 2005

Abstract

The rearrangement of isophorone oxide over Al-MCM-41-type mesostructured catalysts with different Si/Al molar ratios was investigated. The main rearrangement products were the α-diketone and the keto aldehyde, whereas the product coming from the decarbonylation of the latter was detected in minor amounts. The textural properties and the number of acid sites of Al-MCM-41 materials influence the extent of isophorone oxide rearrangement reaction. The best catalytic performance in terms of epoxide conversion was obtained for a catalyst with a molar Si/Al ratio around 40 due to the proper contribution of acid site concentration and pore size. However, irrespective of the aluminium content of the catalysts and the reaction temperature, the selectivity to the desired keto aldehyde was around 80%. Al-MCM-41 materials are superior catalysts compared with zeolites in terms of both activity and aldehyde selectivity. Because of their large pore size, using Al-containing mesostructured materials as catalysts in isophorone oxide rearrangement avoids the diffusional problems present in zeolites.

Keywords: Isophorone oxide; Rearrangement; Epoxide; Mesostructured materials; Al-MCM-41

1. Introduction

The catalytic rearrangement of epoxides, leading to useful intermediates in organic syntheses, has been widely studied over both homogeneous and heterogeneous catalysts [1,2]. Acidic activation of epoxides for ring-opening reactions leading to aldehydes, ketones, ethers, or alcohols can be achieved either by Brönsted acid catalysts via addition of a proton to the epoxide oxygen or by Lewis acid catalysts via coordination of the epoxide oxygen to a multivalent cation [3]. Using zeolitic materials as catalysts for the epoxide rearrangement reactions has the advantage of a well-defined pore system compared with homogeneous systems or other heterogeneous catalysts, such as metal oxides (e.g., silica and alumina), metal sulfates, or precipitated phosphates [4]. Indeed, zeolites in their proton form (e.g., ZSM-5), as well as the weakly Lewis-acidic titanium containing zeolites (e.g., TS-1 and Ti-Beta), have been found to catalyse this type of reaction [5].

Cyclic α,β-epoxy ketones are interesting intermediates in organic synthesis, because they are very reactive compounds. Several products resulting from the rearrangement of such epoxides are valuable raw materials for the preparation of perfumes, synthetic food flavorings, and pharmaceuticals [6,7]. The rearrangement of α,β-epoxy ketones was originally investigated by House et al. using homogeneous Lewis acids as catalysts [8]. The cyclic α,β-epoxy ketones are rearranged via an intramolecular reaction to aldehydes and diones using boron trifluoride etherate as a homogeneous catalyst. In the presence of Lewis acids, the oxirane ring is cleaved at the β-carbon atom, as depicted in Scheme 1. Cleavage at the α-carbon is energetically unfavourable, because it generates partial positive charges on adjacent atoms [9]. Cleavage is followed by acyl migration (route A) or hydrogen migration (route B). Acyl migration results in ring contraction to yield the aldehyde, a reaction pathway favoured over hydrogen migration when $BF_3 \cdot EtO_2$ is used as catalyst, particularly if an additional substituent is present at the β-position [10].

Heterogeneous catalysts have scarcely been used in the rearrangement of α,β-epoxy ketones, despite their advantages in terms of ease of recovery and recycling. Rao and Rao stud-

---

[*] Corresponding author. Fax: +34 91 488 70 68.
E-mail address: juan.melero@urjc.es (J.A. Melero).

0021-9517/$ – see front matter © 2005 Elsevier Inc. All rights reserved.
doi:10.1016/j.jcat.2005.09.028

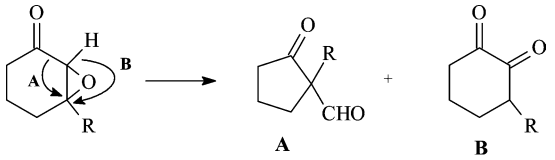

Scheme 1. Lewis acid-catalysed rearrangement of a cyclic α,β-epoxy ketone. (A) Acyl migration, (B) hydrogen migration.

ied the rearrangement of highly active chalcone oxides to 1,3-diphenylpropane-1,2-diones at room temperature using silica gel as a catalyst [11]. Meyer et al. reported liquid- and vapour-phase rearrangement of isophorone oxide with high yields (up to 80%) to keto aldehyde over zeolitic materials [12]. Recently, Elings et al. [13] investigated the rearrangement of various cyclic α,β-epoxy ketones (i.e., isophorone oxide, 2,3-epoxy-3-methylcyclohexan-1-one, and pulegone oxide) with the use of solid acid catalysts, including silica, zeolites, and clays, as an alternative to the classical homogeneous $BF_3 \cdot Et_2O$ system.

Zeolites are microporous materials of limited pore size, producing a strong diffusional hindrance for both reactants and products and thus rapid deactivation. Therefore, in the presence of bulky compounds, the activity of zeolites is restricted to active sites located on the external surface. In this context, compared with zeolites, the mesoporous MCM-41 materials discovered by researchers at Mobil Oil Company [14] may be convenient catalysts in processes involving high-volume molecules, because they have high surface areas and large mesopore diameters. Indeed, the incorporation of Al atoms into the walls turned these materials into solids with acid sites of medium strength, with potential applications for the catalytic conversion of bulky molecules [15,16]. Moreover, these catalysts can be synthesized over a wide range of Si/Al ratios, making it possible to modify and adjust their acidic properties.

Recently, Al-containing MCM-41 materials were reported to be more effective than zeolites and other mesoporous catalysts for both liquid- and vapour-phase Beckmann rearrangement of cyclohexanone oxime [17,18]. Although works dealing with the use of solid acids in Claisen rearrangement are rather scarce, Mathew et al. reported the use of Al-MCM-41 with different Si/Al ratios in the rearrangement of allyl phenyl ether and observed a close relationship between acidity and conversion [19]. Moreover, α-pinene oxide rearrangement to campholenic aldehyde in liquid phase over Al-MCM-41-type mesostructured materials has been documented [20]. In this work high conversion was observed in comparison with other catalysts, such as SiO_2, B_2O_3/SiO_2, and $ZnCl_2$, but selectivity was dependent on the aluminium content, varying from 49 to 66%.

We recently studied the catalytic rearrangement of 1,2-epoxyoctane in liquid phase over different solid catalysts with various acid properties and structural features, including diverse zeolites and mesostructured materials [21,22]. The mesoporous materials presented much higher activities per active site compared with the zeolitic materials, probably due to their larger pore sizes. This previous work prompted us to apply Al-MCM-41-type mesostructured materials as catalysts in the rearrangement of epoxides of varying natures with applications to fine chemistry. In the present paper we report for the first time the catalytic performance of Al-MCM-41 materials with different Si/Al molar ratios on the liquid-phase isophorone oxide rearrangement.

2. Experimental

2.1. Synthesis and characterization of catalysts

Al-containing MCM-41-type catalysts with Si/Al ratios of 5–100 were prepared in our laboratory according to a sol–gel procedure at room temperature described previously [23]. Two solutions were prepared under gentle stirring: solution A, formed by 20 g of tetraethylorthosilicate (TEOS; Alfa) and aluminium isopropoxide (AIP; Aldrich; from 0.2 to 3.9 g depending on the initial Si/Al molar ratio in the synthesis gel), and solution B, formed by 36.5 g of hexadecyltrimethylammonium chloride (CTACl; Aldrich) and 6.6 g of hydrogen chloride. Once these solutions were perfectly homogenised, solution A was added to solution B, and the mixture was kept under stirring at room temperature for 75 min. Thereafter, 54 g of a 2 wt% aqueous ammonia solution was added dropwise and stirred for 1 h. The obtained sample was filtered, washed with deionizated water, and dried at 110 °C for 12 h. The final product was obtained by calcination in static air at 550 °C for 12 h.

The catalytic samples synthesised were characterized by different techniques. Mesoscopic ordering was checked through X-ray diffraction (XRD) patterns acquired with a Philips X′PERT MPD diffractometer using Cu-K_α radiation. Typically, the data were collected from 0.6° to 10° (2θ), with a resolution of 0.02°. The Si/Al atomic ratio of the calcined samples was obtained by inductively coupled plasma–atomic emission spectroscopy with a VARIAN VISTA-AX apparatus. Textural properties of catalysts were determined by means of nitrogen adsorption–desorption isotherms at 77 K with a Micromeritics ASAP 2010 porosimeter after outgassing of the calcined samples under vacuum at 200 °C for 5 h. The surface areas were obtained according to the BET equation, whereas the pore size distribution in the mesopore region was determined by applying the BJH method to the adsorption branch of the isotherm. The total pore volume was calculated from the nitrogen adsorption at $p/p_0 = 0.99$.

The coordination of aluminium atoms in the framework of the solids was checked by ^{27}Al-MAS-NMR spectra of the calcined samples. The spectra were recorded at 104.26 MHz in a VARIAN Infinity 400 spectrometer at spinning frequency of 4 KHz. Intervals of 30 s between successive accumulations were selected. The external standard reference was $[Al(H_2O)_6{}^{+3}]$, and all measurements were carried out at room temperature. Catalyst acidity was determined by ammonia temperature-programmed desorption (TPD) in a Micromeritics 2910 (TPD/TPR) equipment. Previously, the samples were outgassed under a helium flow (50 $\text{Nml}\,\text{min}^{-1}$) at a heating rate of 15 $°\text{C}\,\text{min}^{-1}$ up to 560 °C and kept at this temperature for 30 min. After cooling to 180 °C, an ammonia flow of 35 $\text{Nml}\,\text{min}^{-1}$ was passed through the sample for 30 min. The physisorbed ammonia was removed by flowing helium at 180 °C for 90 min. The desorption of the chemically adsorbed ammonia was monitored while the temperature was increased up to 560 °C at a rate of 15 °C min^{-1} and maintained for 30 min. The ammonia concentration in the effluent stream was measured by means of a thermal conductivity detector.

2.2. Catalytic experiments

The catalytic experiments were carried out at 80 °C in a 0.1-L stirred batch autoclave, equipped with a temperature controller and a pressure gauge under stirring (550 rpm) and autogenous pressure. This experimental setup was also provided with a device to feed the epoxide into the Teflon-lined reactor once the reaction temperature was reached. The solvent and the catalyst are initially placed in the Teflon-lined reactor. The zero time of the reaction is taken when the temperature reaches the setpoint value and the epoxide is loaded into the reactor. The composition of the reaction mixture was as follows: 1.25 g of isophorone oxide, 50 g of toluene (water content <0.03 wt%) and 0.1 g of catalyst. Toluene was stored with zeolite A to minimise its water content. The catalyst, prior reaction, was dried overnight at 140 °C to remove adsorbed water.

The reaction products were analyzed with a VARIAN 3800 gas chromatograph equipped with a capillary column (HP-FFAP) with dimensions 60 × 0.32 mm, using a flame ionization detector. Identification of the different reaction products was performed by mass spectrometry (VARIAN SATURN 2000) using standard compounds.

3. Results and discussion

3.1. Catalyst properties

The main physicochemical and textural properties of the Al-MCM-41 materials prepared in this work are summarized in Table 1. Chemical analysis of calcined samples yielded molar Si/Al ratios higher than those present in the starting synthesis mixture, although the degree of aluminium incorporation was enhanced at low Al content. Starting from a Si/Al molar ratio of 100, the incorporation was ca. 90%, whereas from initial Si/Al molar ratios of 5 and 20, the incorporation decreased to ca. 37 and 50%, respectively. However, a question to be considered is whether this aluminium was tetrahedrally incorporated into the silica framework. As-synthesised materials exhibited a unique signal centred at 50 ppm in the ^{27}Al MAS-NMR spectra, indicating a tetrahedral environment of Al atoms regardless of their content in the synthesis medium. In contrast, ^{27}Al MAS-NMR spectra of the samples after calcination in air at 550 °C exhibited two clear peaks centred at ∼0 and ∼50 ppm originating from octahedrally and tetrahedrally coordinated aluminium species, respectively (Fig. 1). The relative proportion of octahedral aluminium increased as the molar Si/Al ratio of the catalyst decreased, although its contribution was always clearly lower than that corresponding to tetrahedral aluminium for the three samples. These results demonstrate that the incorporation of aluminium atoms in MCM-41 silica walls was hindered as the aluminium content in the synthesis mixture increased.

Table 1
Physicochemical properties of the Al-MCM-41 type catalysts

Catalysts	Al-MCM-41 (1)	Al-MCM-41 (2)	Al-MCM-41 (3)
Si/Al (starting composition)	5	20	100
Si/Al (calcined sample)	14	38	114
D_{BJH} (nm)[a]	<2.0	2.3	2.5
D_p (nm)[b]	1.9	3.0	3.1
Surface area ($m^2 g^{-1}$)	720	1049	1115
Pore volume ($cm^3 g^{-1}$)[c]	0.34	0.78	0.87
Acidity (mmol g^{-1})[d]	0.52	0.23	0.11
$T_{maximum}$ (°C)[d]	266	268	270
Al ($mmol_{Al} g^{-1}$)[e]	1.15	0.43	0.15

[a] Maximum pore size distribution calculated from the adsorption branch using the BJH method.
[b] Pore diameter calculated assuming cylindrical geometry as D_p (nm) = 4 × pore volume ($cm^3 g^{-1}$)/surface area ($m^2 g^{-1}$) × 1000.
[c] Total pore volume measured at $P/P_0 = 0.99$.
[d] Calculated from ammonia TPD measurements.
[e] Total aluminium species per g of calcined sample.

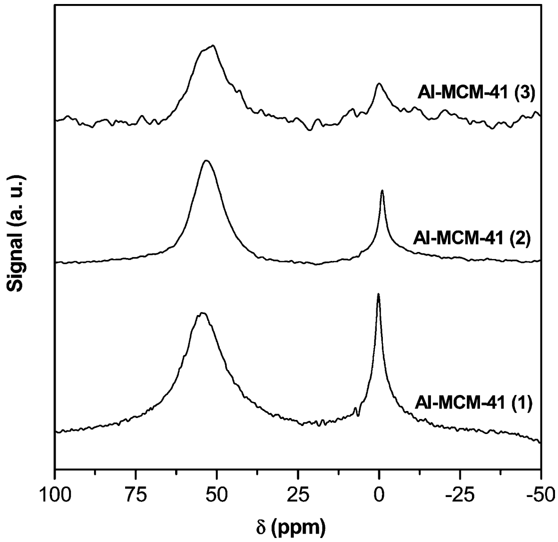

Fig. 1. ^{27}Al MAS-NMR spectra of calcined samples.

For all of the calcined samples, the XRD spectra in Fig. 2 show solely a main peak in the range 2.7–3.5 nm ($2\theta = 3.29$–$2.49°$) corresponding to the d_{100} reflection of 2D hexagonal symmetry with intensity varying slightly with aluminium content. In general, the d-spacing at $2\theta \cong 3°$ decreases with increasing aluminium content ($d = 3.5$, 3.3, and 2.7 nm for Si/Al = 100, 20, and 5, respectively), and less well-resolved XRD patterns are obtained. Additional peaks are not observed, indicating the absence of long-range order. Therefore, larger amounts of aluminium incorporated in the pore walls cause a decrease in the long-range order in Al-containing MCM-41 materials [23].

Fig. 3 exhibits the nitrogen adsorption isotherms at 77 K for the three calcined samples Al-MCM-41 (1), (2), and (3), along with their respective pore size distributions. The Al-MCM-41 (2) and (3) samples have a type IV isotherm in the IUPAC classification, typical for mesoporous materials. Note-

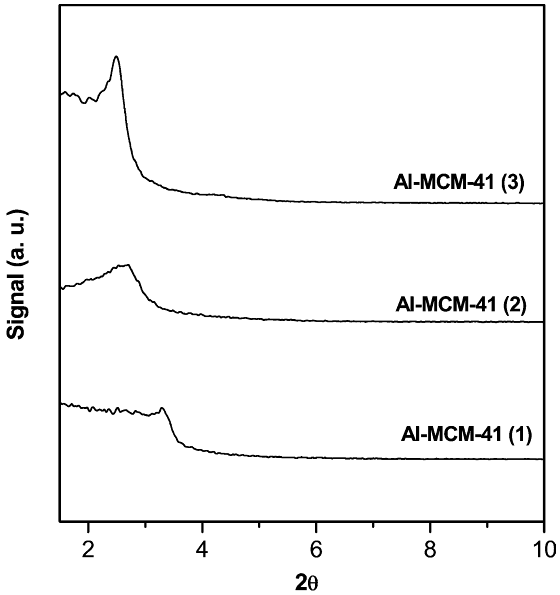

Fig. 2. XRD spectra of calcined samples.

worthy common features in the isotherms of both samples are a mono-multilayer adsorption zone at low relative pressure, a distinct jump of capillary condensation in mesopores at $P/P_0 = 0.1$–0.4, and an almost constant adsorption zone at high relative pressures due to multilayer adsorption on the particle surface. The inflection point of these isotherms is situated at $P/P_0 \sim 0.25$, and the different stages are clearly separated. This is not the case with the adsorption isotherm for the Al-MCM-41 (1) sample, which does not show capillary condensation in the mesopores, just mono-multilayer adsorption or micropore filling. This isotherm can be classified as type I following IUPAC criteria, which is typical for microporous materials. These types of isotherms have been previously reported for MCM-41 materials with small pore sizes, synthesised through a sol–gel route based on the use of short-chain cationic surfactants [24]. The decrease in pore size at high Al content is in agreement with the reduction in the d-spacing observed in the XRD spectra.

BET surface area, pore volume, and average pore size present a common trend, with a continuous increase with increasing molar Si/Al ratio (see Table 1). Thus the BET surface area values increase from 720 to 1115 $m^2\,g^{-1}$, pore volume (measured at $P/P_0 = 0.99$) increases from 0.34 to 0.87 $cm^3\,g^{-1}$, and average pore size increases from <2.0 nm to 2.5 nm. Therefore, the aluminium content has a strong influence on the textural properties of the material finally obtained, because it leads to a change from mesoporous materials, Al-MCM-41 (3) and (2), to a microporous material ($D_p < 2.0$ nm) in the case of the Al-MCM-41 (1) sample.

The acid properties of Al-MCM-41 samples were investigated by NH_3 TPD analysis (Fig. 4); the results are reported in Table 1. As expected, the number of acid sites increased with increasing aluminium content incorporated within the mesoscopic structure. Nevertheless, a number of Al atoms remained inaccessible to ammonia molecules. This accessibility was clearly enhanced with lower Al content in the synthesis mixture, reaching the highest values for the material synthesised with an initial molar ratio of 100. Chemical and NH_3 TPD analysis clearly indicate that low Al content in the synthesis mixture favours the incorporation and accessibility of Al atoms in the mesoscopic structure. All samples demonstrate the presence of sites with medium acid strength, as indicated by the temperature maximum of ammonia desorption within the range 266–270 °C. Regardless of their aluminium content, all of the samples present acid sites of similar strength, at least based on the data obtained from TPD measurements. Additionally, all of the samples also show one or two shoulders in the main signal at temperatures >450 °C, probably arising from dehydroxilation processes promoted at high temperatures.

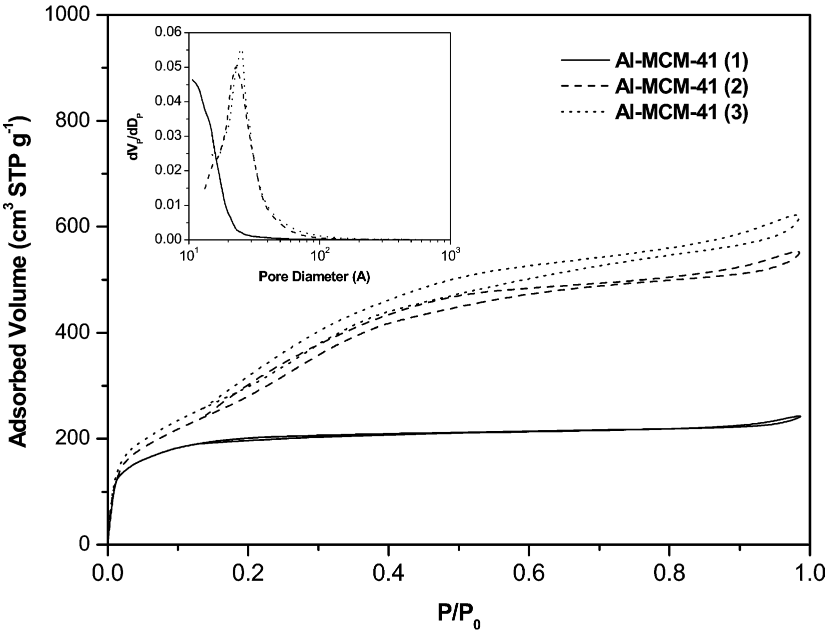

Fig. 3. Nitrogen adsorption isotherms at 77 K and BJH pore size distributions (left top) of calcined samples.

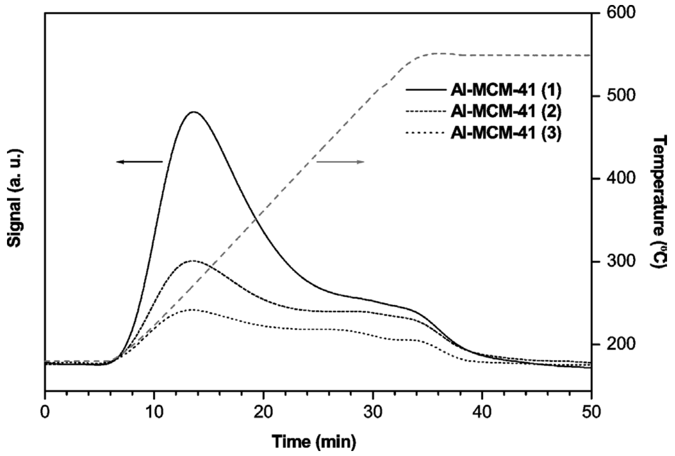

Fig. 4. NH_3 TPD of calcined samples.

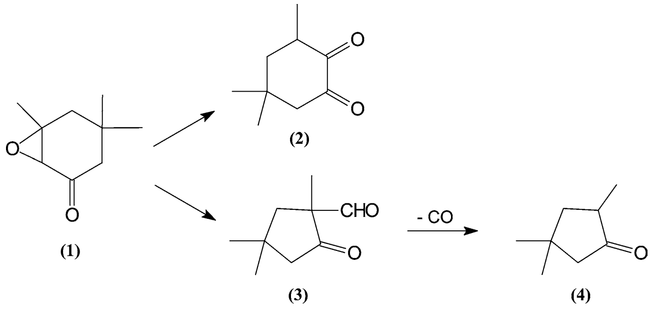

Scheme 2. Rearrangement of isophorone oxide (**1**) to 3,5,5-trimethyl-1,2-cyclohexanedione (**2**) and 2-formyl-2,4,4-trimethylcyclopentanone (**3**) and subsequent deformylation of (**3**) to 2,4,4-trimethylcyclopentanone (**4**).

3.2. *Catalytic epoxide rearrangement*

Rearrangement of isophorone oxide (**1**) yields, as major products, α-diketone (**2**) and keto aldehyde (**3**), whereas the formation of (**4**) can be explained by deformylation of (**3**), as depicted in Scheme 2 [5]. From an industrial standpoint, the desired compound is the keto aldehyde, an interesting intermediate for the synthesis of other cyclopentanone derivatives with floral and fruity smells. The acid-catalysed reaction mechanism leading to the synthesis of keto aldehyde (**2**) has been discussed for homogeneous catalysts [25]. Therefore, it is of interest whether the product distribution changes in the presence of a heterogeneous catalyst system and also whether the decarbonylation of the compound (**3**) to compound (**4**) can be suppressed.

Fig. 5 shows the epoxide conversion results obtained over the different Al-MCM-41 samples in the rearrangement of isophorone epoxide in liquid phase. Because some epoxides may be isomerised thermally, a blank reaction in absence of catalyst was carried out; this yielded a negligible conversion under the reaction conditions used in this work. However, when Al-MCM-41 materials were used as catalysts, epoxide conversion increased significantly with increasing reaction time. The highest values were obtained over Al-MCM-41 (2) material (with a molar Si/Al ratio of 38), for which the epoxide conversion reached approximately 60% during the first 25 min of reaction and increased up to 90% in 2 h.

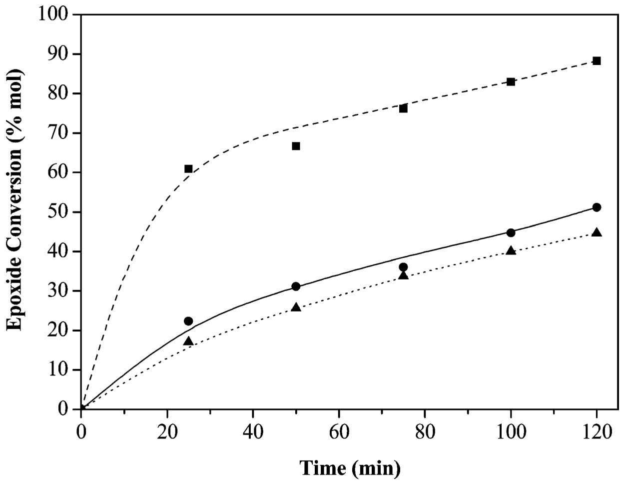

Fig. 5. Epoxide conversion vs. reaction time in the isophorone oxide rearrangement over different Al-MCM-41 at 80 °C. (●) Al-MCM-41 (1), (■) Al-MCM-41 (2), (▲) Al-MCM-41 (3).

The low conversion observed with Al-MCM-41 (1) (molar Si/Al ratio of 14; $D_p < 2.0$ nm) in comparison to that obtained with Al-MCM-41 (2) ($D_p > 2.0$ nm) is presumably due to its lower average pore size, which hinders the accessibility of the epoxide to the active sites of the catalyst and the diffusion of products out of the pore system. The epoxide conversion values obtained over Al-MCM-41 (3) catalyst (molar Si/Al ratio of 114; $D_p > 2.0$ nm) are noteworthy; greater values should have been expected, considering the large pore diameter of this material. These results may be attributed to the lower aluminium content of this catalyst, leading to a decrease of the number of active sites present on its surface. Consequently, the extent of isophorone oxide rearrangement reaction seems to be clearly influenced by textural properties as well as by the number of acid sites present in Al-MCM-41 materials used as catalysts. In this sense, a Si/Al molar ratio of ca. 40 can be considered an optimal aluminium content of the Al-MCM-41 catalyst, allowing the proper combination of pore size and acid site concentration to be attained.

For all the samples, a second reaction stage occurred after 25 min of reaction, in which the reaction rate decreased. This may be attributed to the control of the reaction by the internal diffusion of reactants and products within the mesoscopic channels. In any case, the effect of deactivation of the acid sites by adsorption of organic compounds to explain the decreased activity obtained in this second stage should not be discounted. The high absolute epoxide conversion (ca. 60%) attained for Al-MCM-41 (2) after 25 min of reaction may also explain the marked decrease in activity for this catalyst as a consequence of the substrate disappearance.

Fig. 6 shows the molar product distribution obtained in isophorone epoxide rearrangement over Al-MCM-41 catalysts with varying aluminium content. It is remarkable that, regardless the catalysts used, the main reaction product was 2-formyl-2,4,4-trimethylcyclopentanone (**3**) with selectivity around 80–90%, whereas the selectivity of 3,5,5-trimethyl-1,2-cyclohexanedione (**2**) ranged from 10 to 20%. Conse-

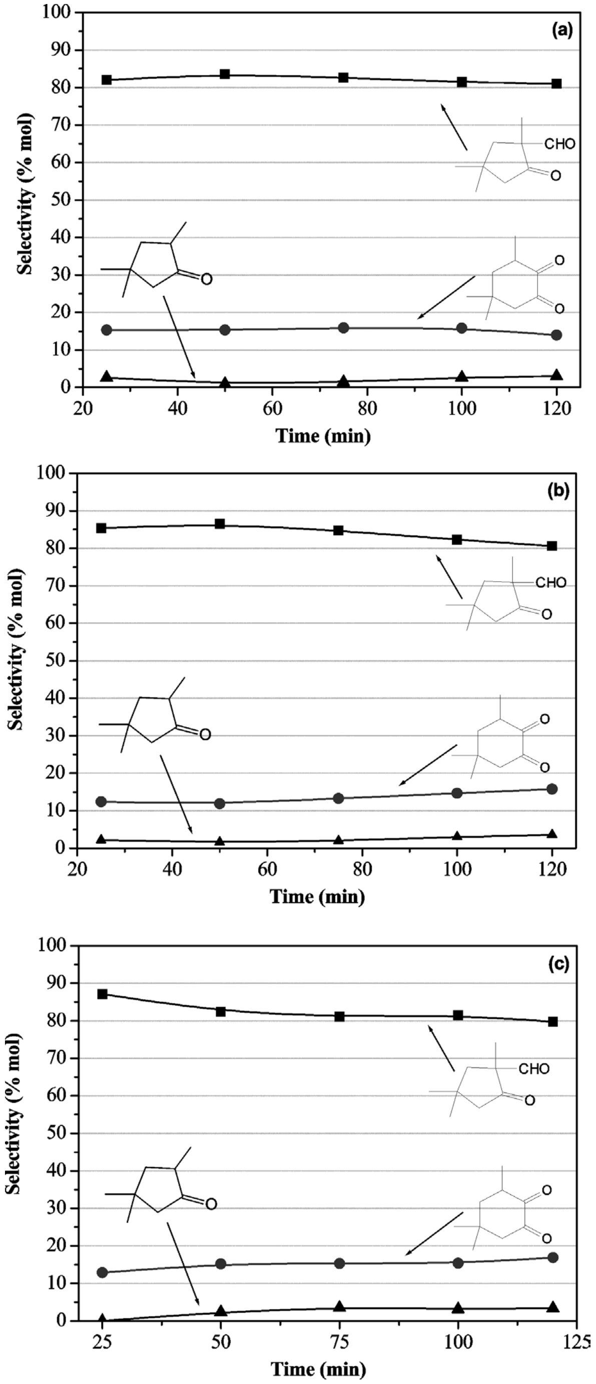

Fig. 6. Molar product distribution obtained in isophorone epoxide rearrangement over Al-MCM-41 type mesostructured materials at 80 °C: (a) Al-MCM-41 (1), (b) Al-MCM-41 (2), (c) Al-MCM-41 (3).

quently, these results indicate that the presence of an additional substituent in the β-position of cyclic α,β-epoxy ketones, such as isophorone oxide, when mesoporous acid materials are used as catalysts, favours acyl migration, resulting in ring contraction and consequently the formation of the aldehyde over hydrogen migration, leading to the α-diketone. Moreover, Al-MCM-41 materials hinder the deformylation of 2-formyl-2,4,4-trimethylcyclopentanone (**3**), because 2,4,4-trimethylcyclopentanone (**4**) selectivities are almost negligible.

Table 2
Effect of reaction temperature on isophorone epoxide rearrangement over Al-MCM-41 (2)

Temperature	Conversion[a] (%)	Selectivity (%)[a]		
		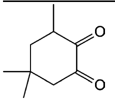 **(2)**	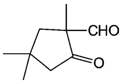 **(3)**	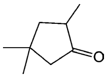 **(4)**
60	29.6	18.9	79.1	2.0
80	60.9	12.4	85.4	2.2
100	87.9	14.1	77.5	8.4

[a] Reaction time = 25 min.

Although conversion was found to be dependent on the Si/Al ratio of the Al-MCM-41 material, reaction product selectivity hardly varied with the varying aluminium content of the catalysts or reaction time. As Fig. 6 shows, selectivity toward the three reaction products detected was similar over the three Al-MCM-41 catalysts tested and varied slightly with the course of the reaction. In this way, selectivity toward 3,5,5-trimethyl-1,2-cyclohexanedione (**2**), 2-formyl-2,4,4-trimethylcyclopentanone (**3**), and 2,4,4-trimethylcyclopentanone (**4**) was set at around 16, 80, and 4%, respectively.

In conclusion, we found that liquid-phase isophorone oxide rearrangement over Al-MCM-41-type mesostructured materials led to high yields (up to 80%) toward keto aldehyde (**3**) after 2 h of reaction, together with low formation of the α-diketone (**2**) and negligible selectivity toward the decarbonylation product (**4**). Considering epoxide conversion, the best catalytic performance was obtained over Al-MCM-41 material with a molar Si/Al ratio of ca. 40. This catalyst combined appropriate pore size and number of acid sites, yielding a 90% epoxide conversion and aldehyde selectivity of ca. 80% after 2 h of reaction.

To study the influence of temperature over the extent of the reaction, isophorone oxide rearrangement was studied over the Al-MCM-41 (2) catalyst at 60, 80, and 100 °C (Table 2). The reaction time was 25 min with the purpose of obtaining comparative epoxide conversions. The main product was 2-formyl-2,4,4-trimethylcyclopentanone (**3**), with selectivity around 80% regardless of temperature, although the results in Table 2 show that the deformylation process seems slightly favoured with temperature increase. As expected, conversion was enhanced with the increase of the temperature. It is remarkable that isophorone epoxide conversion at 100 °C over Al-MCM-41 materials reached values close to 100% for a reaction time of just 25 min with high aldehyde selectivity.

Finally, the results obtained in the present work were compared with those published by Hoelderich et al. [26] in the liquid-phase isophorone oxide rearrangement over zeolitic materials (see Table 3). Most of zeolites tested yielded complete conversion at 110 °C, albeit with long reaction times (6 h). The activity of ZSM-5 and ferrierite is probably related to the acid sites located in the outer surface of the zeolite crystals. Indeed, the external acid sites likely influence the activity demonstrated by all of the zeolites tested.

Although the previous results show that zeolites efficiently catalyse the rearrangement of isophorone oxide to 2-formyl-

Table 3
Liquid-phase rearrangement of isophorone oxide over zeolites (data adapted from [26])[a]

Catalyst	Conversion (%)	Selectivity (%)		
		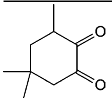 **(2)**	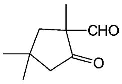 **(3)**	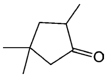 **(4)**
ZSM-5 (28)	88	14	68	1
ZSM-5 (60)	95	15	68	0
Al-BEA (25)	100	13	68	14
USY (70)	96	12	73	0
USY (96)	100	11	74	1
Ferrierite (18)	100	12	81	0

[a] Reaction conditions: $t = 6$ h; $T = 110\,°\mathrm{C}$; solvent: toluene; loading: 10 g isophorone oxide/g catalyst. The numbers in parentheses correspond to the SiO_2/Al_2O_3 ratios.

2,4,4-trimethylcyclopentanone, it is worthwhile to compare them with the catalytic results obtained in this work using Al-MCM-41 materials as catalysts. Molar product distributions obtained over Al-MCM-41 (**2**) catalyst at different temperatures (see Table 2) show that Al-containing mesostructured materials yield high selectivities to the valuable product keto aldehyde (**3**), with values even higher to those obtained over ferrierite and USY zeolites. Moreover, Al-MCM-41 materials present much higher activity, yielding isophorone epoxide conversions close to 100% under reaction conditions similar to those used with zeolites (100 °C; toluene as solvent; 12.5 g isophorone oxide/g catalyst), but with very short reaction times (25 min). These results can be assigned to the larger pores of mesostructured materials that avoid the diffusional problems present in zeolitic catalysts.

4. Conclusions

Al-MCM-41 materials effectively catalyse isomerisation of isophorone oxide toward 2-formyl-2,4,4-trimethylcyclopentanone, which is an useful compound for the synthesis of perfumes and synthetic flavours. Epoxide conversion is directly related to the pore size and amount of acid sites of Al-MCM-41 catalysts. A Si/Al molar ratio of ca. 40 is an optimal value, combining an appropriate number of acid sites and pore diameters. For all of the catalysts, selectivity toward the aldehyde decreases slightly with increasing reaction time, with values of ca. 80% obtained after 2 h of reaction. The temperature affects epoxide conversion, but does not significantly modify the product distribution. The aluminium-containing mesostructured catalysts display high activity and selectivity toward the aldehyde isomer compared with zeolitic materials.

References

[1] J. Marc, Advanced Organic Chemistry, Wiley, New York, 1985.
[2] K. Arata, K. Tanabe, Bull. Chem. Soc. Jpn. 53 (3) (1980) 299.
[3] J.G. Buchanan, H.Z. Sable, Selective Organic Transformations, Wiley, New York, 1972.
[4] W.F. Hölderich, H. van Bekkum, Stud. Surf. Sci. Catal. 137 (2001) 821.
[5] W.F. Hölderich, in: R.A. Sheldon, H. van Bekkum (Eds.), Fine Chemicals Through Heterogeneous Catalysis, Wiley/VCH, Weinheim, 2001, p. 217.
[6] T.-L. Ho, S.-H. Liu, Synth. Commun. 13 (1983) 685.
[7] M. Asaoka, S. Hayashibe, S. Sonoda, H. Takei, Tetrahedron 47 (1991) 6967.
[8] H.O. House, J. Am. Chem. Soc. 76 (1954) 1235;
H.O. House, R.L. Wasson, J. Am. Chem. Soc. 78 (1956) 4394;
H.O. House, R.L. Wasson, J. Am. Chem. Soc. 79 (1957) 1488;
H.O. House, G.D. Ryerson, J. Am. Chem. Soc. 83 (1961) 979.
[9] H.O. House, D.J. Reif, R.L. Wasson, J. Am. Chem. Soc. 79 (1957) 2940.
[10] R.D. Bach, M.W. Tubergen, R.C. Klix, Tetrahedron Lett. 27 (1986) 3565.
[11] T.B. Rao, J.M. Rao, Synth. Commun. 23 (1993) 1527.
[12] C. Meyer, W. Laufer, W.F. Hölderich, Catal. Lett. 53 (1998) 131.
[13] J.A. Elings, H.E.B. Lempers, R.A. Sheldon, Stud. Surf. Sci. Catal. 105 (1997) 1165;
J.A. Elings, H.E.B. Lempers, R.A. Sheldon, Eur. J. Org. Chem. (2000) 1905.
[14] C.T. Kresge, M.E. Leonowicz, W.J. Roth, J.C. Vartuli, J.S. Beck, Nature 359 (1992) 710.
[15] A. Corma, A. Martínez, V. Martínez-Soria, J.B. Montón, J. Catal. 153 (1995) 25.
[16] D.P. Serrano, J. Aguado, J.L. Sotelo, R. van Grieken, J.M. Escola, J.M. Menéndez, Stud. Surf. Sci. Catal. 117 (1998) 437.
[17] C. Ngamcharussrivichai, P. Wu, T. Tatsumi, J. Catal. 227 (2004) 448.
[18] L. Forni, C. Tosi, G. Fornasari, F. Trifirò, A. Vaccari, J.B. Nagy, J. Mol. Catal. A: Chem. 221 (2004) 97.
[19] N.T. Mathew, S. Khaire, S. Mayadevi, R. Jha, S. Sivasanker, J. Catal. 229 (2005) 105.
[20] D.B. Ravindra, Y.T. Nie, S. Jaenicke, G.K. Chuah, Catal. Today 96 (2004) 147.
[21] D.P. Serrano, R. van Grieken, J.A. Melero, A. García, Appl. Catal. A: Gen. 269 (2004) 137.
[22] R. van Grieken, D.P. Serrano, J.A. Melero, A. García, J. Mol. Catal. A: Chem. 222 (2004) 167.
[23] J. Aguado, D.P. Serrano, J.M. Escola, Microporous Mesoporous Mater. 34 (2000) 43.
[24] D.P. Serrano, J. Aguado, J.M. Escola, E. Garagorri, Chem. Commun. (2000) 2041.
[25] R.D. Bach, R.C. Klix, Tetrahedron Lett. 26 (1985) 985.
[26] C. Meyer, W. Laufer, W. Hölderich, Catal. Lett. 53 (1998) 131.